IECON 2024 - 50th Annual Conference of the IEEE Industrial Electronics Society | 978-1-6654-6454-3/24/$31.00 ©2024 IEEE | DOI: 10.1109/IECON55916.2024.10905302

Design and Fabrication of Wearable Sensors for the Measurement of Ammonia Concentration in Air

Andrew R. Hall [1], Nathan Hose [1], Harris Nakajima [1], Seong-Joong Kahng [2], Jae-Hyun Chung [2], Igor Novosselov [2], Christopher Simpson [3] and Alexander Mamishev [1]

[1] Department of Electrical and Computer Engineering, University of Washington, Seattle, United States
[2] Department of Mechanical Engineering, University of Washington, Seattle, United States
[3] Department of Environmental and Occupational Health Sciences, University of Washington, Seattle, United States

Abstract*—Exposure to emissions from combustion, farming, and industrial processes triggers asthma, cardiovascular disease, and lung inflammation. One of the primary goals for environmental surveillance and health-related research is developing a low-cost and high-performance wearable sensing platform that can accurately measure concentrations of gaseous pollutants, toxic industrial chemicals, and other chemical compounds that adversely affect human health. Specifically, occupational exposure to ammonia is significant for janitorial workers, miners, and agricultural workers, and the health effect of exposure to low ammonia levels (<1 ppm) is unknown because there are no wearable ammonia sensors sensitive enough for this type of measurement. This paper introduces a novel opto-electrostatic sensing mechanism that utilizes single-walled carbon nanotubes (SWCNTs) to fabricate lightweight sensors capable of detecting ammonia concentrations as low as 100 ppb. The high sensitivity of Nafion-doped SWCNTs makes them superior to commercially available sensors at a cost significantly lower than that of laboratory-grade analyzers. By directly addressing the shortcomings of existing sensor technology, our work positions portable ammonia sensors to improve safety standards in industries utilizing ammonia.

***Index Terms*— Ammonia Sensor, Nafion, Carbon Footprint, Single-walled Carbon Nanotubes SWCNTs, Energy Efficiency**

I. Introduction

The significance of monitoring gaseous pollutants spans multiple areas vital to the environment and human health. Using flexible, low-cost sensors in many applications has significant advantages over more expensive gas analyzers. Specifically, occupational exposure to ammonia (NH_3) is significant for janitorial workers, miners, and agricultural workers. The hazards are exacerbated in rural pediatric populations because children are likely more susceptible to ammonia exposure, and the exposure duration is more significant in the farm environment. The extent of the hazards of low ammonia levels (below one ppm) is unknown because there are no wearable ammonia sensors sensitive enough for this type of measurement. Existing sensor technologies face high cost, limited selectivity, and large size.

These advantages benefit sensor networks, where measurements must be taken at multiple locations and for personal exposure monitoring. High-sensitivity and selectivity sensors for personal exposure monitoring are of interest to epidemiological studies, to individuals who are sensitive to air quality (e.g., asthma patients and people with severe allergies), or for use in hazardous occupational environments.

Recent advancements in low-cost particulate matter (PM) sensors led to their extensive use in various applications, such as air quality (AQ) monitoring in indoor [1] and outdoor [2] environments, including large-scale deployments. Various studies have evaluated the performance of low-cost sensors in laboratory and field settings [3], showing that low-cost sensors yield usable data when calibrated against research-grade reference instruments [4]. The low-cost sensor networks have the potential to provide high spatial and temporal resolution, identifying pollution sources and hotspots, which in turn can lead to the development of intervention strategies for exposure assessment and intervention strategies for susceptible individuals. Time-resolved exposure data from wearable monitors can be used to assess individual exposure in near real-time [5]. A hybrid approach combining indoor, outdoor, and wearable low-cost air quality sensors was recently used to evaluate the effectiveness of intervention strategies [6]. While the research on human PM exposure has been growing rapidly, catalyzed by the development of robust, low-cost sensors, the studies related to ammonia exposure and related health effects could not be performed as low-cost ammonia sensors have not yet been developed. We aim to create a high-sensitivity and specificity sensor to enhance safety in industries where ammonia exposure poses significant health risks.

Scientific literature shows that exposure to gaseous pollutants can trigger diseases, including asthma, cardiovascular disease, and significant lung inflammation [7]. For example, occupational exposure to NH_3 is significant for janitorial workers, miners, and agricultural workers [8]. The OSHA permissible exposure limit for NH_3 is 50 ppm (8 hrs. exposure); however, recent studies show respiratory effects with NH_3 exposures at 2 ppm, resulting in increased prevalence of respiratory symptoms and impaired lung function in farmworkers exposed to ammonia and in residents of rural communities exposed to sub-ppm concentrations of ammonia emitted by animal agriculture [7, 9].

Asthma affects 24.6 million people in the US (2009 estimate), including 9.6% of children, and shows a particularly high prevalence among poor children (13.5%) and non-Hispanic black children (17.0%) [10]. Asthma accounts for more than 4,000 deaths per year in the US [11]. The estimated annual direct, productivity, and mortality costs of asthma in the US are enormous, estimated at $56 billion (2007) [12]. Long-term asthma surveillance data are challenging to interpret, but asthma prevalence increased from the 1980s through the 1990s and continued to rise in the 2000s [11].

Recent advances in nanomaterial research led to the development of novel sensor platforms. Among nanomaterial gas sensors, carbon-based materials, including amorphous carbon, CNTs, and graphene sheets, are very popular due to their well-developed synthesis methods and well-characterized detection mechanisms [13]. Single-wall carbon nanotubes (SWCNTs) are more sensitive than graphene because their effective density of states around the Fermi level is lower than that of graphene [14]. The rolled structure of SWCNTs provides greater edge effects than that of the planar structure of graphene, which contributes to the superior sensing performance of SWCNTs. Since the first demonstration of a CNT gas-sensing mechanism [15], sensors for detecting various gas molecules have been proposed. In SWCNTs, doping polymers, such as PEI or Nafion, could enhance the sensor's sensitivity and specificity. The non-functionalized SWCNTs could be selective only to negatively charged targets, such as NO_2. SWCNTs doped with negatively charged Nafion could be selective to positively charged gas, such as ammonia. This selectivity originates from the electrostatic interaction between the polymer and gas molecules in their excited state. The positively charged polymer binds with negatively charged gas molecules, increasing an SWCNT sensor's selectivity. This paper presents a non-contact capillary-bridge-induced printing method that allows continuous SWCNT lines without damaging the substrate or the previously printed layers [16].

The method is superior to other commercially available techniques. The contact current printing method can be used for CNT printing; however, damages the substrate and impedes printing multiple layers, which is critical for fabricating functionalized sensors [17]. Inkjet-style printing [18] is the most common method in non-contact printing. Thermal expansion or electromechanical vibration ejects droplets, which overcomes surface tension in the formation of the droplets. Due to the physics of droplet formation, inkjet printing is limited to the range of viscosities and surface tension of the working fluid [17]. The non-contact capillary method deposits nano-ink through a liquid bridge between the capillary pen and substrate. Consequently, the capillary pen does not damage the substrate.

The literature points out the novel technologies used in developing sensors based on the carbon materaials [19] and hybrid sensors [20]. The sensing mechanisms include chemo resistive [21], capacitive [22], surface acoustic wave [23], electrochemical [24], and others. However, compared to PM air quality sensors, the low-cost ammonia did not reach a wide commercial application and further research is needed to advance technology towards practical application.

This paper introduces an innovative opto-electrostatic sensing paradigm that utilizes single-walled carbon nanotubes (SWCNTs) to fabricate lightweight sensors capable of detecting ammonia concentrations as low as 100 ppb. The high sensitivity of Nafion-doped SWCNTs makes them superior to commercially available sensors while maintaining a cost significantly lower than that of laboratory-grade analyzers.

II. Experimental

A. Sensor Fabrication

The fabrication process will take advantage of Single-Walled Continuous Nanotubes (SWCNT), cylindrical structures with a single layer of carbon atoms. They have a high surface area-to-volume ratio and unique electronic properties, making them useful in various applications, including gas detection sensors [25]. This paper uses a variant of Kahng's method [16] to deposit SWCNTs onto a PET substrate, doping the SWCNTs with Nafion. In the previous study, the team developed a non-contact capillary-bridge-induced printing method that allows for the printing of continuous SWCNT lines without damaging the substrate or the previously printed layers . The non-contact capillary method deposits nanoink through a liquid bridge that forms between the capillary pen and substrate, allowing for the printing of complex sensor geometries without damaging previous layers and introducing the doping required for selective sensing.

The printing method is illustrated in Fig. 1, where a Fig. 1a demonstrates the liquid bridge that forms between the capillary bridge and substrate, Fig. 1b shows the printing setup, Fig. 1c the illustrates the printing procedure, and Fig. 1d shows the printing technique used for the fabrication of the gas sensor.

This method is superior to other commercially available techniques. For example, contact printing methods [25] can be

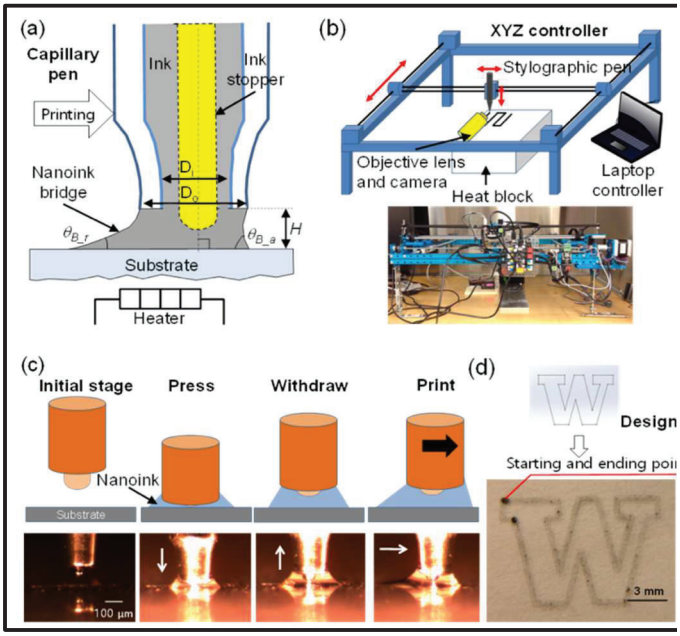

Fig. 1. *Nanoink capillary printing (a) Concept (b) Schematic of an XYZ plotter installed with a heating stage and an imaging system. (c) Nanoink-bridge-induced printing using water ink on a PET film. (d) W-pattern printed by SWCNT-ink.*

used for CNT printing; however, this damages the substrate [26] and impedes the printing of multiple layers, which is critical for fabricating functionalized sensors. Inkjet-style printing is the most common method in non-contact printing [26]. Thermal expansion or electromechanical vibration ejects droplets, which overcome surface tension in the formation of the droplets [26]. Due to the physics of droplet formation, inkjet printing is limited to the range of viscosities and surface tension of the working fluid [27]. The non-contact capillary method deposits nanoink through a liquid bridge that forms between the capillary pen and substrate.

In sensor fabrication, SWCNTs (5 mg/ml) were first mixed with 1% sodium dodecyl sulfate (SDS) via sonification. Mixing SWCNTs with SDS increases the SWCNTs' uniformity. After the SDS sonification, a PET film was placed on a 100°C hotplate. Next, a micropipette was used to drop 5 µl of the SWCNT-SDS solution onto the PET film. The SWCNTs were patterned as a line on the film (refer to Fig. 2). After patterning the SWCNTs, the film was cured on the hotplate for 10 minutes. After curing, the film was removed from the hotplate, and then silver paste was stamped to the sides of the SWCNT line for electrical contact (refer to Fig. 2).

After applying the silver paste, the film was cured on an 80°C hotplate for 30 minutes. After curing the silver paste, the PET film was removed from the hotplate. Then, 5 µl of 0.1% Nafion (Nafion 117 solution, Sigma-Aldrich Co, LLC.) was deposited on the SWCNT pattern (refer to Fig. 2). After depositing the Nafion, the film was cured on a 100°C hotplate for 1 hour.

B. Experimental Setup

The sensor's response to NH_3 was evaluated in a 0.036 m^3 acrylic environmental chamber (Cleantech, Orange, CA) situated inside a fume hood. The environmental chamber's gas concentration was regulated by a mass flow control system. This control system was used to deliver the desired concentration of NH_3 and air to the environmental chamber. The NH_3 and air were purchased from Praxair. A Picarro G2103 cavity ring down gas analyzer (Picarro, Santa Clara, CA) was used as a reference instrument to verify NH_3 concentrations in the environmental chamber. Fig. 3 shows the system diagram and experimental setup.

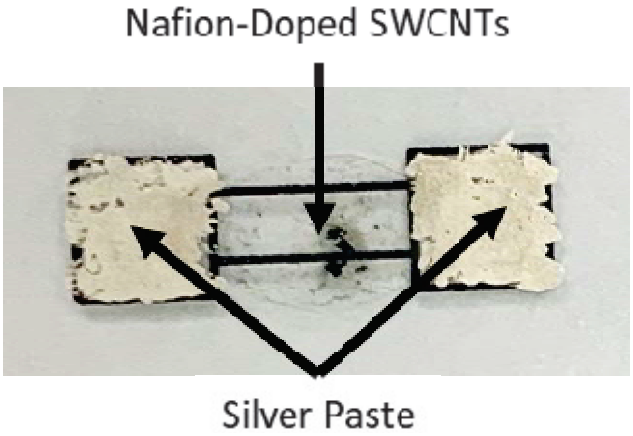

Fig. 2. The PET film outline. The SWCNTs were deposited in the center of the outline. Then, the SWCNTs were doped with Nafion. Finally, silver paste was stamped onto the sides of the outline to provide electrical contact.

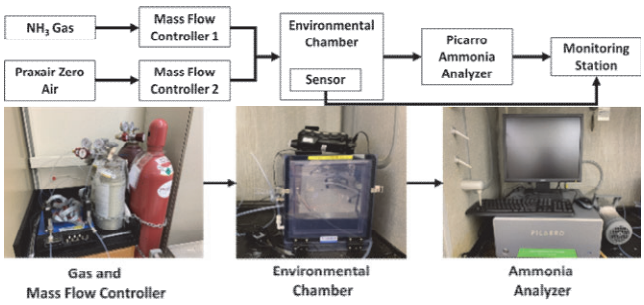

Fig. 3. Experimental setup. The mass flow controller regulated the gas' output into the environmental chamber, which was monitored by the NH_3 analyzer.

The resistance of the sensor was measured using a voltage divider circuit (Fig. 4). The voltage divider's reference resistance was chosen to be as close as possible to the sensor's baseline resistance, which allows for high-resolution data.

The voltage divider was powered by an Arduino Uno's 5-volt power supply. The Arduino Uno recorded the sensor's voltage-based signals through an analog pin. The Uno converted the voltage signal into the sensor's resistance according to (1):

$$R_{Sense} = R_{Ref}\left(\frac{V_{in}}{V_{out}} - 1\right) \quad (1)$$

where R_{Sense} is the resistance of the sensor, R_{Ref} is the resistance of the reference resistor in the voltage divider circuit, V_{In} is the DC voltage supplied to the sensor, and V_{Out} is the voltage read by the Arduino microcontroller. After processing the signal, the Uno transmitted the data to a computer for future analysis.

C. Procedure

The sensing circuit was situated inside the environmental chamber. Then, the environmental chamber was continuously filled with ultra-high purity air to remove the residual ammonia and possible contaminants from the chamber. As a result, this procedure also ensured that the relative humidity (RH) inside the chamber was 0%. This low RH allows the sensor to isolate

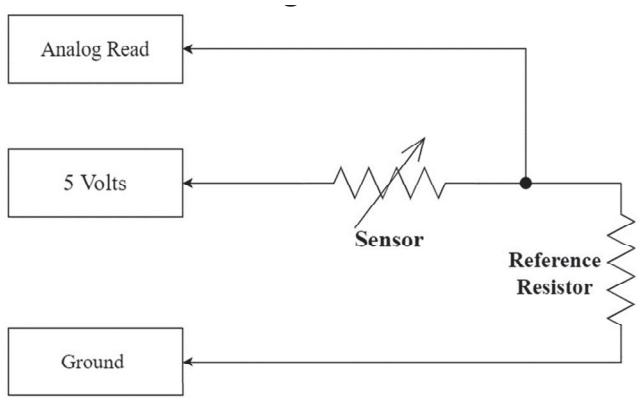

Fig. 4. Voltage divider. The voltage divider's reference resistance was chosen to be as close as possible to the sensor's baseline resistance, which allows for high-resolution data. The voltage divider was powered by an Arduino Uno's 5-volt power supply.

ammonia and not be affected by interferants. Once the RH read 0%, NH_3 was flooded into the environmental chamber until the analyzer read 100 ppb. The 100 ppb of NH_3 was held constant until the sensor's resistance achieved a stable value. Once the sensor response stabilized, the NH_3 was turned off, and the chamber flooded with zero air until the sensor's resistance approached its baseline value. This sensor calibration process was repeated for 200, 500, and 1,000 ppb of NH_3. The sensor response is compared to the ammonia analyzer Picarro G2103 cavity ring down gas analyzer to verify NH_3 concentrations.

III. Results and Discussion

A. SWCNT Sensitivity

Fig. 5 and Table 1 displays the data collected from the SWCNT sensor for three different step increases in ammonia concentration. The sensor's response is plotted according to (2):

$$\overline{R_{out}} = \overline{R_{Sense}} - \min\left(\overline{R_{Sense}}\right) \quad (2)$$

where R_{Sense} is the set that contains all the measured resistances of the sensor, and R_{Out} is the set plotted in Fig. 6. The SWCNT sensor shows a response to less than 100 ppb of ammonia while demonstrating the ability to predict a wide range of NH_3 concentrations. The sensor's resistances, according to (2), are 100 Ω, 390 Ω, 680 Ω, and 1,200 Ω when exposed to NH_3 concentrations of 125 ppb, 325 ppb, 590 ppb, and 1,100 ppb, respectively. Moreover, the sensor showed linearity for all the NH_3 concentrations that were tested. Fig. 7 displays the regression curve of the sensor, showing that the sensor has an R^2 value of 0.99.

While the sensor shows extreme sensitivity to NH_3, the sensor's baseline resistance drifts after every NH_3 cycle. This drift is attributed to NH_3 being an adhesive gas, meaning the NH3 molecules tend to adsorb into materials in the sensing environment. Therefore, the sensor will still produce a response to NH_3 when NH_3 is depleted from the sensing chamber's environment. To fix this drift problem, heat could be applied to the surface of the sensor to force the NH_3 molecules to desorb from the sensor [28].

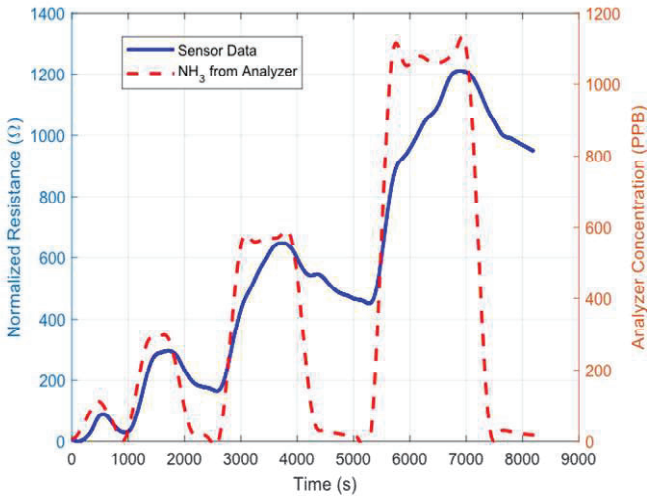

Fig. 6. SWCNT sensitivity to ammonia. The sensor can detect ammonia concentrations lower than 100 ppb while also capable of sensing ammonia concentrations higher than 1 ppm.

B. Sensor Response Time

The response times of the SWCNT sensor are shown in Fig. 5a) through c), are magnified versions of Fig. 6 that clearly shows the sensor's 10%, 50%, and 90% response times. Fig. 5a) shows the response of the sensor after getting exposed to 100- ppb of NH_3. At 100 ppb concentration of NH_3, the sensor takes close to 4.5 minutes to produce a noticeable response, which is also the point at which the sensor's resistance is 10% of its maximum. Furthermore, the sensor initially drops in resistance after exposure to NH_3 gas. The probable cause of this decrease in resistance is due to a transient increase in temperature that was introduced when the NH_3 was first inserted into the environmental chamber.

This resistance decrease was not observed at any other NH_3 concentration. Furthermore, the SWCNT sensor reached its 50% and 90% maxima at 6 minutes and 7.75 minutes, respectively, when exposed to 100 ppb. Moreover, Fig. 5b) and Fig. 5c) display the sensor's response to 300 ppb and 600 ppb of ammonia, respectively. Fig. 5 shows the sensor's resistance change at different concentrations of NH_3. At each concentration, 10%, 50%, and 90% of the maximum resistance

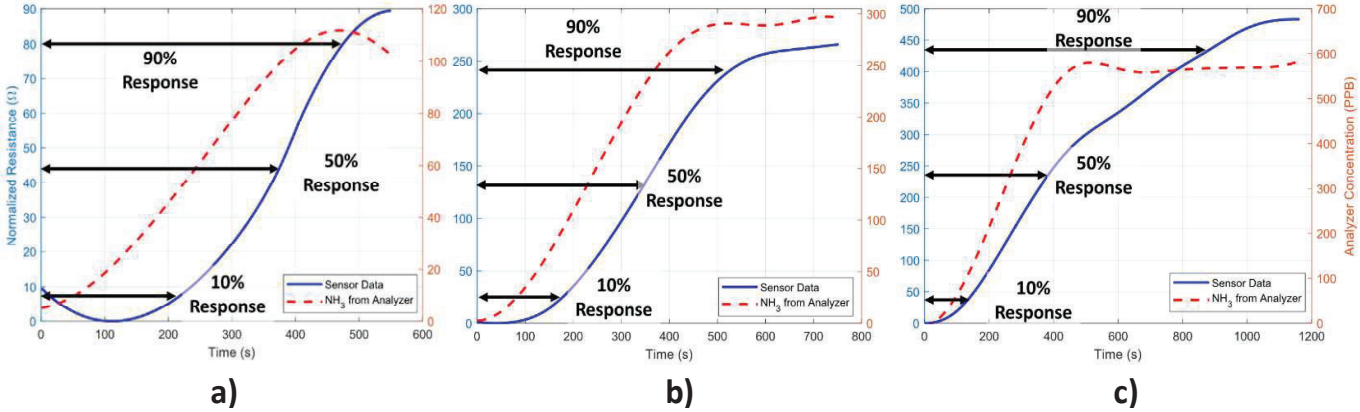

Fig. 5. Response time of the SWCNT sensors when exposed to a) 100 ppb, b) 300 ppb, and c) 600 ppb of ammonia. There are no initial drops in the sensor readings when ammonia is introduced to the sensing environment, meaning that the drop for a) may be attributed to incipient recombination mechanisms occurring in the SWCNTs.

Table 1. RESISTANCE CHANGE AT DIFFERENT CONCENTRATIONS OF AMMONIA.

Percent of Maximum Response (%) / Ammonia Concentration (PPB)	10		50		90	
	Time to Reach (Minutes)	Resistance Change (Ω)	Time to Reach (Minutes)	Resistance Change (Ω)	Time to Reach (Minutes)	Resistance Change (Ω)
100	3.6	9 Ω	6.2	45 Ω	7.7	81 Ω
300	2.9	27 Ω	5.9	133 Ω	8.5	240 Ω
600	2.9	48 Ω	6.4	242 Ω	13.9	435 Ω
1100	3	76 Ω	3	380 Ω	20.5	680 Ω

values are recorded. Generally, the sensor took a longer time to reach its 10% point when exposed to lower concentrations of NH_3. However, the sensor took a shorter time to reach its 90% point when exposed to lower concentrations of NH_3. The group theorized that at high concentrations of NH_3, gas adsorption, and desorption compete with each other, which leads to the sensor reaching its equilibrium state at an extended time [29].

IV. CONCLUSION AND FUTURE WORK

In this paper, we demonstrated the construction of an NH_3 sensor based on a novel Opto-electrostatic sensing approach that utilizes the unique properties of single-walled carbon nanotubes (SWCNTs) doped with Nafion. Our results show an NH_3 detection level of less than 100 ppb, representing a significant improvement of 100 times compared to low-cost gas monitors typically used for monitoring ammonia in workplaces [30]. Moreover, the sensor demonstrated linearity at different NH3 concentration levels, an important property that allows the sensor's readings to be easily interpretable.

Our future work will address the relatively long response time that the Nafion-doped SWCNT showed by exposing the sensor to a UV light source or using a different combination of SWCNTs and Nafion. Additionally, we plan to test the sensor's selectivity in the presence of interfering gases, followed by miniaturizing the sensor into a wearable device that will be field-tested and evaluated.

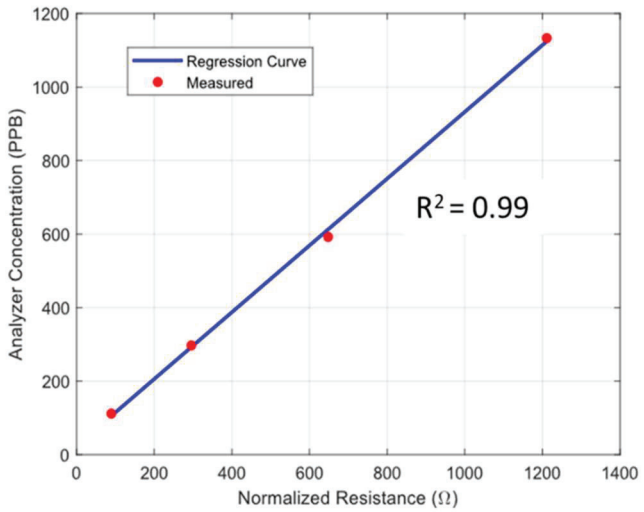

Fig. 7. The linear regression curve of the sensor. The analysis found that the sensor's response has an R2 value of 0.99. Hence, the sensor is highly linear.

ACKNOWLEDGMENT

This work was supported by the National Institute of Environmental Health Sciences (grant number P30ES007033) and the National Institute of Occupational Safety and Health (grant number R21OH011364). The authors thank Edmund Y. W. Seto for supplying the environmental chamber, mass flow controllers, and lab space. The authors also thank Chaofan Deng, Tyler Darby, and Cindy Imm for helping with the experimental setup, sensor fabrication, and calibration testing.

REFERENCES

[1] S. Makhsous, J. M. Segovia, J. He, D. Chan, L. Lee, I. V. Novosselov, and A. V. Mamishev, "Methodology for Addressing Infectious Aerosol Persistence in Real-Time Using Sensor Network," *Sensors,* vol. 21, no. 11, pp. 3928, 2021.

[2] E. Seto, E. Austin, I. Novosselov, and M. G. Yost, "Use of low-cost particle monitors to calibrate traffic-related air pollutant models in urban areas."

[3] M. Zusman, C. S. Schumacher, A. J. Gassett, E. W. Spalt, E. Austin, T. V. Larson, G. Carvlin, E. Seto, J. D. Kaufman, and L. Sheppard, "Calibration of low-cost particulate matter sensors: Model development for a multi-city epidemiological study," *Environment International,* vol. 134, pp. 105329, 2020.

[4] C.-Y. Chao, H. Zhang, M. Hammer, Y. Zhan, D. Kenney, R. V. Martin, and P. Biswas, "Integrating Fixed Monitoring Systems with Low-Cost Sensors to Create High-Resolution Air Quality Maps for the Northern China Plain Region," *ACS Earth and Space Chemistry,* vol. 5, no. 11, pp. 3022-3035, 2021.

[5] G. E. Duncan, E. Seto, A. R. Avery, M. Oie, G. Carvlin, E. Austin, J. H. Shirai, J. He, B. Ockerman, and I. Novosselov, "Usability of a personal air pollution monitor: Design-feedback iterative cycle study," *JMIR mHealth and uHealth,* vol. 6, no. 12, pp. e12023, 2018.

[6] J. He, C.-H. Huang, N. Yuan, E. Austin, E. Seto, and I. Novosselov, "Network of low-cost air quality sensors for monitoring indoor, outdoor, and personal PM2.5 exposure in Seattle during the 2020 wildfire

season," *Atmospheric Environment,* vol. 285, pp. 119244, 2022/09/15/, 2022.

[7] C. Loftus, M. Yost, P. Sampson, E. Torres, G. Arias, V. B. Vasquez, K. Hartin, J. Armstrong, M. Tchong-French, S. Vedal, P. Bhatti, and C. Karr, "Ambient Ammonia Exposures in an Agricultural Community and Pediatric Asthma Morbidity," *Epidemiology,* vol. 26, no. 6, pp. 794-801, Nov, 2015.

[8] B. Bakke, B. Ulvestad, Y. Thomassen, T. Woldbæk, and D. G. Ellingsen, "Characterization of occupational exposure to air contaminants in modern tunnelling operations," *Annals of Occupational Hygiene,* vol. 58, no. 7, pp. 818-829, 2014.

[9] M. L. Cantuaria, H. Suh, P. Løfstrøm, and V. Blanes-Vidal, "Characterization of exposure in epidemiological studies on air pollution from biodegradable wastes: Misclassification and comparison of exposure assessment strategies," *International Journal of Hygiene and Environmental Health,* vol. 219, no. 8, pp. 770-779, 2016.

[10] C. Centers for Disease, and Prevention, "Vital signs: asthma prevalence, disease characteristics, and self-management education: United States, 2001--2009," *MMWR Morb Mortal Wkly Rep,* vol. 60, no. 17, pp. 547-52, May 6, 2011.

[11] J. E. Moorman, R. A. Rudd, C. A. Johnson, M. King, P. Minor, C. Bailey, M. R. Scalia, L. J. Akinbami, C. Centers for Disease, and Prevention, "National surveillance for asthma--United States, 1980-2004," *MMWR Surveill Summ,* vol. 56, no. 8, pp. 1-54, Oct 19, 2007.

[12] S. B. Barnett, and T. A. Nurmagambetov, "Costs of asthma in the United States: 2002-2007," *J Allergy Clin Immunol,* vol. 127, no. 1, pp. 145-52, Jan, 2011.

[13] N. Nath, A. Kumar, S. Chakroborty, S. Soren, A. Barik, K. Pal, and F. G. de Souza Jr, "Carbon nanostructure embedded novel sensor implementation for detection of aromatic volatile organic compounds: an organized review," *ACS omega,* vol. 8, no. 5, pp. 4436-4452, 2023.

[14] M. He, S. Zhang, and J. Zhang, "Horizontal single-walled carbon nanotube arrays: Controlled synthesis, characterizations, and applications," *Chemical Reviews,* vol. 120, no. 22, pp. 12592-12684, 2020.

[15] J. Kong, N. R. Franklin, C. W. Zhou, M. G. Chapline, S. Peng, K. J. Cho, and H. J. Dai, "Nanotube molecular wires as chemical sensors," *Science,* vol. 287, no. 5453, pp. 622-625, Jan, 2000.

[16] S.-J. Kahng, C. Cerwyn, B. M. Dincau, J.-H. Kim, I. V. Novosselov, M. Anantram, and J.-H. Chung, "Nanoink bridge-induced capillary pen printing for chemical sensors," *Nanotechnology,* vol. 29, no. 33, pp. 335304, 2018.

[17] S.-J. Kahng, "Wearable Carbon Nanotube Sensors: Fabrication and Applications for Bio/Chemical Sensors," 2019.

[18] M. A. Shah, D.-G. Lee, B.-Y. Lee, and S. Hur, "Classifications and applications of inkjet printing technology: A review," *IEEE Access,* vol. 9, pp. 140079-140102, 2021.

[19] X. Tang, M. Debliquy, D. Lahem, Y. Yan, and J.-P. Raskin, "A review on functionalized graphene sensors for detection of ammonia," *Sensors,* vol. 21, no. 4, pp. 1443, 2021.

[20] S. Singh, S. Sharma, R. C. Singh, and S. Sharma, "Hydrothermally synthesized MoS2-multi-walled carbon nanotube composite as a novel room-temperature ammonia sensing platform," *Applied Surface Science,* vol. 532, pp. 147373, 2020.

[21] W. Na, J. Kim, Y. K. Kim, S. G. Kim, and J. Jang, "Fluorination of shape-controlled porous carbon nanoweb layers for ammonia gas sensor applications," *Carbon,* vol. 165, pp. 185-195, 2020.

[22] C. Wu, L. Han, J. Zhang, Y. Wang, R. Wang, and L. Chen, "Capacitive ammonia sensor based on graphene oxide/polyaniline nanocomposites," *Advanced Materials Technologies,* vol. 7, no. 7, pp. 2101247, 2022.

[23] S. Kim, K.-H. Lee, J.-Y. Lee, K.-K. Kim, Y.-H. Choa, and J.-H. Lim, "Single-walled carbon nanotube-based chemi-capacitive sensor for hexane and ammonia," *Electronic Materials Letters,* vol. 15, pp. 712-719, 2019.

[24] H. Ryu, D. Thompson, Y. Huang, B. Li, and Y. Lei, "Electrochemical sensors for nitrogen species: A review," *Sensors and Actuators Reports,* vol. 2, no. 1, pp. 100022, 2020.

[25] J. Kaur, K. Anand, K. Anand, and R. C. Singh, "WO.sub.3 nanolamellae/reduced graphene oxide nanocomposites for highly sensitive and selective acetone sensing," *Journal of Materials Science,* vol. 53, pp. 12894+, 2018.

[26] B. Kang, H. Min, U. Seo, J. Lee, N. Park, K. Cho, and H. S. Lee, "Directly Drawn Organic Transistors by Capillary Pen: A New Facile Patterning Method using Capillary Action for Soluble Organic Materials," *Advanced Materials,* vol. 25, no. 30, pp. 4117-4122, Aug, 2013.

[27] C. Ru, J. Luo, S. Xie, and Y. Sun, "A review of non-contact micro- and nano-printing technologies," *Journal of Micromechanics and Microengineering,* vol. 24, no. 5, May, 2014.

[28] X. Tang, J.-P. Raskin, N. Kryvutsa, S. Hermans, O. Slobodian, A. N. Nazarov, and M. Debliquy, "An ammonia sensor composed of polypyrrole synthesized on reduced graphene oxide by electropolymerization," *Sensors and Actuators B: Chemical,* vol. 305, pp. 127423, 2020.

[29] D. Kwak, Y. Lei, and R. Maric, "Ammonia gas sensors: A comprehensive review," *Talanta,* vol. 204, pp. 713-730, 2019.

[30] E. E. Fabian, "Ammonia Monitoring in Barns Using Simple Instruments," PennState Extension, 2023.

IECON 2024 - 50th Annual Conference of the IEEE Industrial Electronics Society | 978-1-6654-6454-3/24/$31.00 ©2024 IEEE | DOI: 10.1109/IECON55916.2024.10905189

IECON 2024- 50th Annual Conference of the IEEE Industrial Electronics Society

Proceedings

Sheraton Grand Chicago Riverwalk

Chicago, Illinois, USA
3 - 6 November 2024

Sponsored by

IEEE Industrial Electronics Society (IES)

IEEE Catalog Number: CFP24IEC-ART
ISBN: 978-1-6654-6454-3